ACS APPLIED MATERIALS & INTERFACES

Research Article

www.acsami.org

Pure Inorganic Separator for Lithium Ion Batteries

Meinan He,[†] Xinjie Zhang,*[,‡] Kuiyang Jiang,[‡] Joe Wang,[‡] and Yan Wang*[,†]

[†]Mechanical Engineering, Worcester Polytechnic Institute, 100 Institute Road, Worcester, Massachusetts 01609, United States

[‡]Novarials Corporation, 3-H Gill Street, Suite 200, Woburn, Massachusetts 01801, United States

ABSTRACT: Battery safety is critical for many applications including portable electronics, hybrid and electric vehicles, and grid storage. For lithium ion batteries, the conventional polymer based separator is unstable at 120 °C and above. In this research, we have developed a pure aluminum oxide nanowire based separator; this separator does not contain any polymer additives or binders; additionally, it is a bendable ceramic. The physical and electrochemical properties of the separator are investigated. The separator has a pore size of about 100 nm, and it shows excellent electrochemical properties under both room and high temperatures. At room temperature, the ceramic separator shows a higher rate capability compared to the conventional Celgard 2500 separator and life cycle performance does not show any degradation. At 120 °C, the cell with the ceramic separator showed a much better cycle performance than the conventional Celgard 2500 separator. Therefore, we believe that this research is really an exciting scientific breakthrough for ceramic separators and lithium ion batteries and could be potentially used in the next generation lithium ion batteries requiring high safety and reliability.

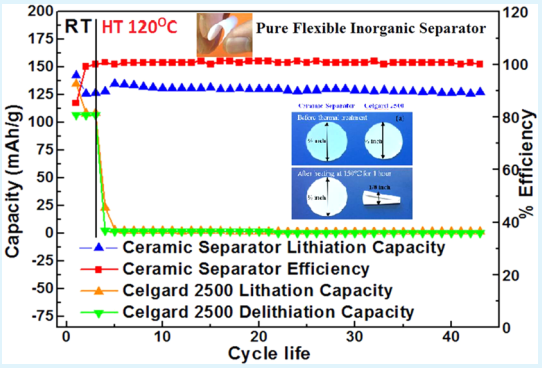

KEYWORDS: *inorganic separator, thermostability, Li-ion batteries*

INTRODUCTION

Lithium ion batteries have dominated the portable electronics market and will potentially dominate large applications including hybrid and electric vehicles, and grid storage because of their high energy and power densities as well as long life cycle. Typically, lithium ion batteries can only be operated at temperatures up to 65 °C due to the limitation of their electrolyte and separator.[1−5] However, high temperature performance is technologically important for many applications such as hybrid and electrical vehicles, aerospace and power-grids.[6−11] The separator is considered as a key safety component of the battery,[12,13] because it directly isolates the anode and cathode. One of the challenges associated with the high temperature use of lithium ion batteries is that the organic separator is unstable at temperatures at 120 °C or above.

A conventional lithium ion battery separator is made of organic polymers including polypropylene (PP), polyethylene (PE), etc., because of their attractive mechanical strength and electrochemical stability. Due to their nonpolar properties, polymer separators suffer from a poor wettability.[14,15] Additionally, poor thermal shrinkage results from the low melting point and glass transition temperature of polymer. Therefore, much research is underway to explore separators with high thermal-resistance and good wettability.[16−18]

One possible solution is to develop an inorganic particle based separator, in which a fine porous structure is combined with ultrafine inorganic particles, such as Al_2O_3, SiO_2, and MgO.[8,19] Inorganic particle based separators have good wettability and very high surface area due to the fine ceramic particles as well as good high temperature performance. It is well-known that both shrinking and melting of the separator in a lithium ion battery would lead to physical contact between the electrodes, which can cause a short circuit. This would not only result in the failure of the cell but also generate heat and cause serious safety problems.

Although inorganic particle based separators offer excellent wettability and extremely thermal stability, they are very brittle. It easily causes cracks during cell winding and assembling. The cracks will lead to a direct contact between the anode and cathode, and the failure of the cell. To solve the problems associated with inorganic particle based separators, composite separators, which combining ceramic particles and polymers are being developed to improve the flexibility and strength. For example, Lee et al. developed Al_2O_3 particles coated polyimide nanofiber separator;[20] Wang et al. synthesized a porous Al_2O_3 particle-PVDF composite separator to solve the brittle problem;[21] Shinet et al. use polyethylene to improve the performance of the ceramic particle based separator;[22] Degussa et al. developed a series of Separion (a trade name) separators by combining the characteristics of polymeric nonwoven and ceramic nanoparticles.[23] However, the operation temperature of the composite separator is significantly reduced because of the polymer. Furthermore, the wettability of composite separator is not as good as pure ceramic separators because of the changing in surface polarity. Moreover, the synthesis method is normally complex because of the adding of new

Received: October 16, 2014
Accepted: December 2, 2014
Published: December 2, 2014

   dx.doi.org/10.1021/am507145h | ACS Appl. Mater. Interfaces 2015, 7, 738−742

compounds. Here, we report a pure ceramic separator made with Al_2O_3 nanowires, which offers high wettability, porosity, good mechanical strength, and exceptional electrochemical performance. The ceramic separator shows an excellent cycle performance at both room temperature and high temperature. With a fine and uniform ceramic nanowire structure, this novel separator is able not only to overcome the problems of ceramic particle based and polymer separators but also to provide a completely new methodology for manufacturing bendable ceramic separators for other applications.

EXPERIMENTAL SECTION

Material Synthesis. The alumina nanowires were prepared by hydrothermal treatment of aluminum-containing precursor at elevated temperature (100 to 180 °C) in a pressure vessel for 12 h, and the nanowire membranes were fabricated by a filtration procedure. Thickness was controlled by adjusting the amount of nanowire used. The wet membranes were then dried and cut for battery assembly. The thickness of the ceramic separator is ~50 μm.

Sample Characterization. Scanning electron microscope (SEM) (JEOL JSM-7000F) and transmission electron microscope (TEM) (Tecnai T12) were used to characterize the morphology of the separator. XRD studies used only the Kα1 component of Cu radiation. An accelerating voltage of 45 kV, current of 40 mA, and scan step of 0.05 were selected.

Electrochemical Measurements. Each composite cathode, including $LiFePO_4$ (LFP), super C_{65}, and polymer binder (2.5 wt % polyvinylidene fluoride) with a weight ratio of 8:1:1 was pasted on the Al foil directly. The thickness of the electrode was around 60 μm. After 120 °C and 2 h vacuum drying, the cathode was cut into $^1/_4$ in. diameter to assemble the cell. The electrochemical testing was against Li foil anode in a Swagelok cell with stainless steel current collectors. The cell was sealed with pressure to ensure good contact. During the room temperature test, 1 M $LiPF_6$ electrolyte was put in a solution of ethylene carbonate (EC), diethyl carbonate (DEC), and dimethyl carbonate (DMC). The ratio of EC, DEC, and DEC was 4:2:4. During the high temperature test, 0.5 M LiBOB dissolved in propylene carbonate (PC) was used as the electrolyte. Cells were tested with a galvanostat/potentiostat/impedance analyzer (Biologic VMP3). CC–CV (Constant Current-Constant Voltage) charging was used, with constant currents applied until cell voltage reached 4.2 V. Each cell was discharged to 2.5 V. The ionic conductivity was tested by soaking 1 layer separator between two stainless steel plate electrodes and evaluated using the electrochemical impedance spectroscopy (EIS) measurement. The applying AC voltage was 20 mV and the amplitude in the frequency was set from 1 mHz to 100 kHz.

In the first step of measuring electrolyte uptake, the initial weight (W_o) of the separator was obtained before the separator was soaked in the electrolyte solution. After being soaked for 1 h, the separator was taken out and the extra electrolyte was removed by the filtering and the electrolyte-infiltrated separator was weighed (W_1). In the end, separators were stored in oven at 50 °C. The weight (W_x) of the separator was recorded at some interval. Typically, the electrolyte uptake and retention of the separator are calculated by the following equations:[30]

$$\text{Electroylte uptake} = \frac{W_1 - W_0}{W_0}$$

$$\text{Electroylte retention} = \frac{W_x - W_0}{W_0}$$

RESULTS AND DISCUSSION

Sample Morphology. Figure 1a shows that Al_2O_3 nanowires based separator is bendable, which is impressive. Figure 1b is the XRD pattern of the ceramic separator and peaks are consistent with those of the gamma-AlOOH

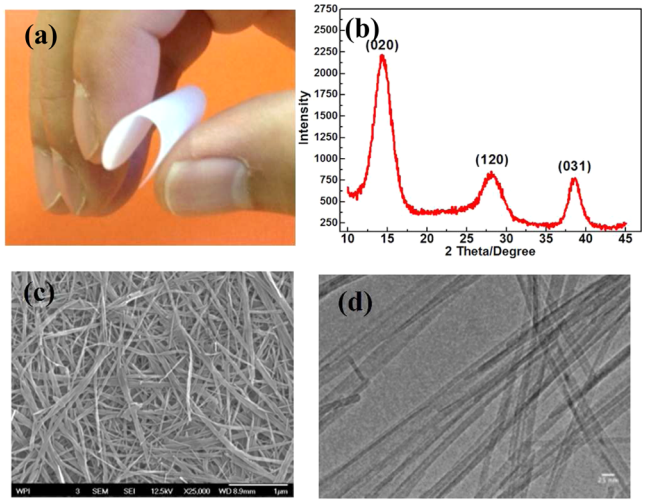

Figure 1. Characterization of the ceramic separator. (a) Diagram of the flexible ceramic separator. (b) XRD pattern of the ceramic separator. (c) SEM micrograph of the ceramic separator. (d) TEM micrograph of the ceramic separator.

(Boehmite) phase with no preferred orientation.[31] In atmosphere, Al_2O_3 nanowire converts to AlOOH due to absorbing water.[32] From Figure 1c, the average diameter of the ceramic nanowire is around 50 nm and the nanowires are uniform and fine. Moreover, the separator exhibited nanosized pores, approximately 100 nm, which are irregularly formed among the ceramic nanowires. The nanowires are bonded to each other at their junctions to form the separator. Due to the homogeneous structure and uniform porous distribution, the separator can absorb much more electrolyte than the polymer one. As a result, good wettability and ion transport of this novel structure are expected. Figure 1d shows the TEM image of a nanowire whose diameter is around 50 nm, which is consistent with SEM results.

Electrochemical Test. The electrochemical properties of the ceramic separator are shown in Figure 2. Figure 2a is the CV curve and the scanning voltage is between 2.5 V and 4.2 V, which is same as the working voltage of the electrochemical cell. A single pair of oxidation and reduction peaks is observed for the sample. It exhibits an anodic peak around 3.6 V and a corresponding cathodic response at 3.3 V, and these peaks can match the characteristic peaks of the $LiFePO_4$/Li foil well.[33] Within this range, no other peaks were observed. Therefore, there are no side reactions for the ceramic separator within the working voltage range and an electrochemical stable environment can be ensured. The mismatch for the first cycle is due to the formation of the SEI layer.[7]

The ionic conductivity of separator was determined by the electrochemical impedance spectroscopy, which was described in previous reports.[15,16,24,25] Figure 2b shows the Nyquist plots for both liquid electrolyte-soaked Celgard 2500 separator and ceramic separator. The ionic conductivity can be calculated by the equation: $\sigma = L/AR$, where L, A, and R are the thickness and area of the separator and the total resistance of the electrolyte across the separator, respectively. The results show that the ionic conductivity of the ceramic based separator was $\sigma = L/AR$ = 50 μm/(1.266 cm^2 × 2.3 Ω × 10 000 μm/cm) = 0.017 s/cm, 1.7 × 10^{-3} S/cm, which was higher than that of Celgard 2500 $\sigma = L/AR$ = 25 μm/(1.266 cm^2 × 2.1 Ω × 10 000 μm/cm) = 0.0009 s/cm, 9 × 10^{-4} S/cm. From the SEM

dx.doi.org/10.1021/am507145h | ACS Appl. Mater. Interfaces 2015, 7, 738–742

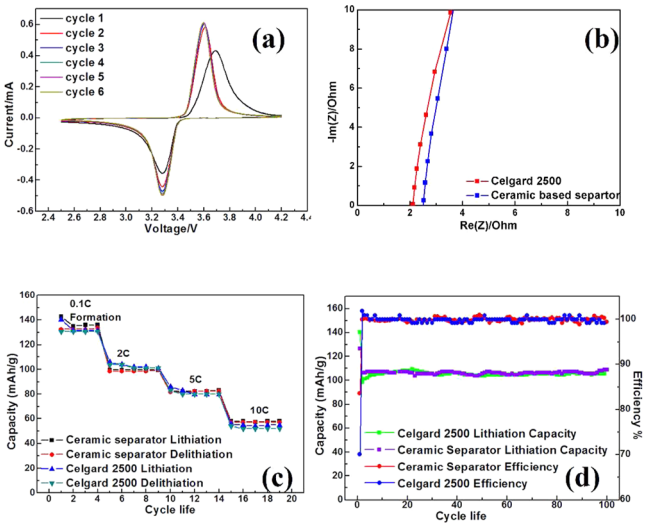

Figure 2. Electrochemical performance of the separator. (a) Cyclic voltammetry curves of the ceramic separator in the potential window of 2.5−4.2 V collected at a rate of 0.1 mV/s. (b) Electrochemical impedance spectroscopy (EIS) plot for the ceramic separator and Celgard 2500 by applying an AC voltage of 20 mV amplitude in the frequency range of 1 mHz−100k Hz. (c) Rate capability for ceramic separator and Celgard 2500. (d) Reversible lithiation capacity and Coulombic efficiency of the ceramic separator and Celgard 2500 versus cycle number under the rate of 2C.

images, there are many interconnected pores in the separator; the porous structure and polar chemical composition of the ceramic nanowire based separator led to a higher porosity and ionic conductivity.[12,26]

Figure 2c shows the rate capabilities of the cell with the ceramic separator and Celgard separator. For the ceramic separator, at 0.1C, the specific capacity is ∼140 mAh/g and with the increasing rate, the specific capacity drops, which is typical for electrochemical cells. The capacity retention ratio is ∼77%, 61%, and 46% at 2 °C, 5 °C, and 10 °C, respectively. We compared the rate performance results of ceramic separator with the conventional polymer separator. It shows that the ceramic based separator has a similar rate capability compared to the conventional polymer separator. Also the coloumbic efficiency is very close to 100% after the first few cycles.

Figure 2d compares the cycle performance of the ceramic separator and polymer separator. The reversibility of the first cycle for the Celgrad 2500 and ceramic separator is 71% and 80%, respectively. It is known that the large drop in the first cycle is due to the formation of the SEI layer.[7] As discussed above, the ceramic separator has a better wettability, which leads to a better contact with electrodes and lower interfacial resistance and higher reversibility. Within the first 10 cycles, the specific capacity of $LiFePO_4$ with Celgard 2500 increases from 100 to 110 mAh/g. With more cycles, the Celgard separator is completely wetted and the specific capacity tends to stabilize. Although we already rested the cell for 1 h before running it, it is not sufficient for complete wetting and a lower ionic conductivity as well as specific capacity is observed for the polymer separator. However, for the ceramic separator, the capacity is stable at ∼110 mAh/g in the second cycle because it absorbed enough electrolytes within 1 h and reached ideal ionic conductivity and specific capacity at the beginning stage. This can be significant for the lithium ion battery industry. With the ceramic separator, the formation and manufacturing time for lithium ion batteries can be greatly shortened, which can potentially decrease the manufacturing time and lower the battery cost.

Figure 3 compares the electrochemical properties for ceramic separator and polymer separator at high temperature. Figure 3a

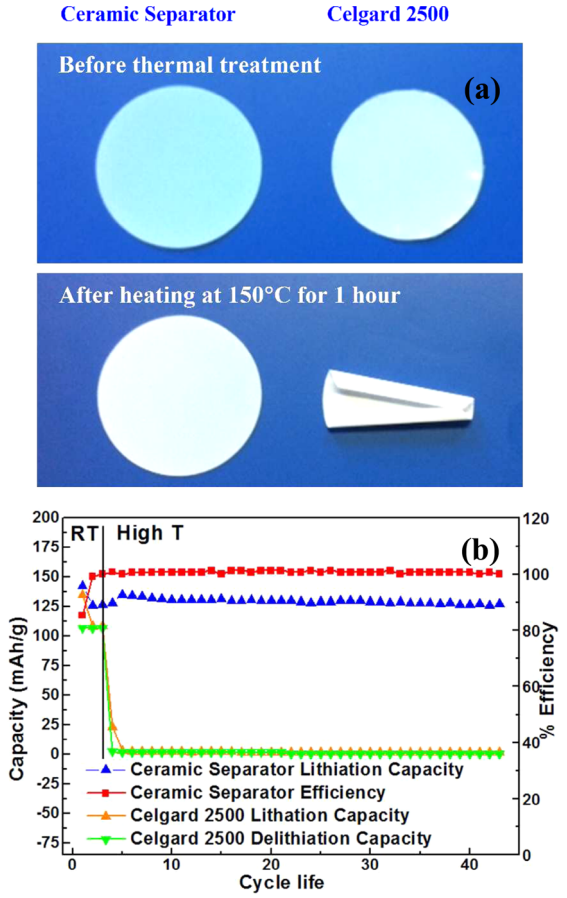

Figure 3. High temperature performance of the separator. (a) Thermal stability comparison of the Celgard 2500 and ceramic separator. (b) Delithiation capacity and Coulombic efficiency of the ceramic separator or Celgard 2500 versus cycle number under room temperature (25 °C) and high temperature (120 °C).

shows the images of the ceramic separator and Celgard 2500 separator before and after thermal treatment at 150 °C for 1 h. It can be seen that the Celgard 2500 separator exhibited significant shrinkage and curved up after the thermal treatment, while the ceramic separator retained its original dimensions. Actually, even if the temperature is increased to 700 °C, the ceramic separator does not show any dimensional changes.

Since the maximum stable working temperature for ethylene carbonate (EC)-diethyl carbonate (DEC)-dimethyl carbonate (DMC) electrolyte is 60 °C, a high temperature electrolyte, 0.5 M LiBOB/propylene carbonate (PC), was used and cells were tested in an oven at 120 °C. Three cycles were run at high temperature to make sure the cells worked well before conducting high temperature tests. From Figure 3b, under room temperature, the ceramic based separator showed a much higher capacity than Celgard 2500. The cell with ceramic separator exhibited an excellent charge−discharge performance at 120 °C for 40 cycles. Compared with the electrochemical properties at room temperature, an increased capacity was observed at 120 °C for the ceramic separator. This is because

dx.doi.org/10.1021/am507145h | ACS Appl. Mater. Interfaces 2015, 7, 738−742

the Li ion diffusivity increases with temperature. However, for the polymer separator, the capacity of the cell drops to almost zero in the first cycle at 120 °C, which is due to the thermal shrinkage of the microspores of Celgard at such a high temperature. Therefore, the results clearly shows that the ceramic based separator has a much stable thermal stability than the commercial polymer separator.

The electrolyte uptake behavior is closely related to ionic conductivity and the electrolyte retention property. It affects the safety and cycle life of the cell significantly.[27] From Figure4,

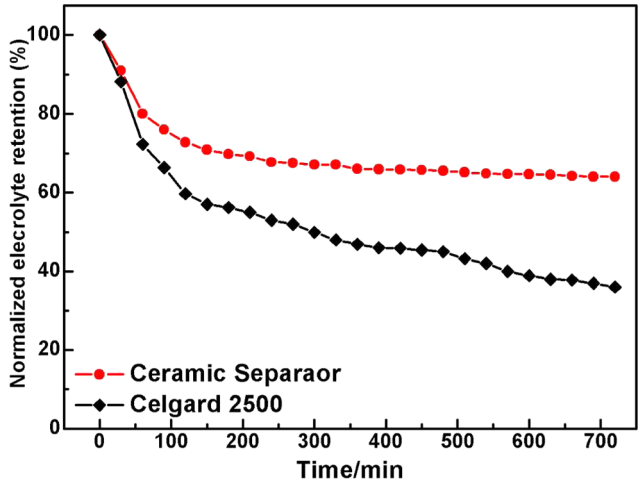

Figure 4. Time dependence of the electrolyte retention for the ceramic separator and Celgard 2500 at 50 °C.

the electrolyte uptake of the Celgard 2500 is determined to be 132%, while the electrolyte uptake for the prepared ceramic separator reached 190%, which is much higher than that of the polymer separator. This is attributed to the high porosity and fine nanostructure. Compared with the Celgard 2500, the retaining ability of liquid electrolyte of the ceramic separator is obviously enhanced. Due to an outstanding porosity and high surface area discussed before, the ceramic separators enhance the interaction between separator and electrolyte, which leads to a higher electrolyte retention.[28,29]

CONCLUSION

In summary, we have successfully fabricated pure flexible ceramic separators, which exhibit outstanding rate capability and cycle life at both room and high temperatures. The ceramic separator showed higher ionic conductivities than that of Celgard 2500 because of its high porosity and better electrolyte uptake/retention properties. Moreover, the ceramic separator shows an attractive thermostability under high temperature electrochemical performance. These advantages allow the ceramic based separator to be potentially used in the next generation lithium ion batteries requiring high thermal stability, safety, and reliability.

AUTHOR INFORMATION

Corresponding Authors

*E-mail: yanwang@wpi.edu.

*E-mail: xzhang@novarials.com.

Author Contributions

M.H., X.Z., and Y.W. designed the experiments. X.Z., J.W., and K.J. fabricated the inorganic separator. M.H. and Y.W. conducted material and electrochemical testing. M.H. and Y.W. analyzed the data. M.H., X.Z., and Y.W. wrote the manuscript.

Notes

The authors declare no competing financial interest.

ACKNOWLEDGMENTS

This research is supported with funding from National Science Foundation (NSF) under contract IIP-1315343. Correspondence and requests for materials should be addressed to Y.W. and X.Z.

REFERENCES

(1) Xu, K.; Zhang, S.; Jow, T. R.; Xu, W.; Angell, C. A. *Electrochem. Solid-State Lett.* **2012**, *5*, A26−A29.
(2) Balakrishnan, P. G.; Ramesh, R.; Prem Kumar, T. *J. Power Sources* **2006**, *155*, 401−414.
(3) Jiang, W.; Liu, Z.; Kong, Q.; Yao, J.; Zhang, C.; Han, P.; Cui, G. *Solid State Ionics* **2013**, *232*, 44−48.
(4) Arora, P.; Zhang, Z. *Chem. Rev.* **2004**, *104*, 4419−4462.
(5) Dunn, B.; Haresh, K.; Tarascon, J.-M. *Science* **2011**, *334*, 928−935.
(6) Cho, T.-H.; Tanaka, M.; Onishi, H.; Kondo, Y.; Nakamura, T.; Yamazaki, H.; Tanase, S.; Sakai, T. *J. Power Sources* **2008**, *181*, 155−160.
(7) Meinan, H.; Sa, Q.; Liu, G.; Wang, Y. *ACS Appl. Mater. Interfaces* **2013**, *5*, 11152−11158.
(8) Scrosati, B. *Electrochim. Acta* **2000**, *45*, 2461−2466.
(9) Etacheri, V.; Marom, R.; Elazari, R.; Salitra, G.; Aurbach, D. *Energy Environ. Sci.* **2011**, *4*, 3243−3262.
(10) Sun, C.; Rajasekhara, S.; Goodenough, J. B.; Zhou, F. *J. Am. Chem. Soc.* **2011**, *133*, 2132−2135.
(11) Nam, D.-H.; Lim, S.-J.; Kim, M.-J.; Kwon, H.-S. *RSC Adv.* **2013**, *3*, 16102−16108.
(12) Jeong, H.-S.; Noh, J. H.; Hwang, C.-G.; Kim, S. H.; Lee, S.-Y. *Macromol. Chem. Phys.* **2010**, *211*, 420−425.
(13) Gwon, H.; Hong, J.; Kim, H.; Seo, D.-H.; Jeon, S.; Kang, K. *Energy Environ. Sci.* **2014**, *7*, 538−551.
(14) Choi, J.-H.; Jegal, J.; Kim, W.-N. *J. Membr. Sci.* **2006**, *284*, 406−415.
(15) Choi, N.-S.; Lee, Y. M.; Park, J. H.; Park, J.-K. *J. Power Sources* **2003**, *119*, 610−616.
(16) Zhang, J.; Yue, L.; Kong, Q.; Zhihong, L.; Zhou, X.; Zhang, C.; Pang, S.; Wang, X.; Yao, J.; Cui, G. *J. Electrochem. Soc.* **2013**, *160*, A769−A774.
(17) Scrosati, B.; Hassoun, J.; Sun, Y.-K. *Energy Environ. Sci.* **2011**, *4*, 3287−3295.
(18) Scrosati, B.; Garche, J. *J. Power Sources* **2010**, *195*, 2419−2430.
(19) Huang, K.-L.; Holsen, T. M.; Chou, T.-C.; Selman, J. R. *Environ. Sci. Technol.* **2003**, *37*, 1992−1998.
(20) Lee, J.; Lee, C.-L.; Park, K.; Kim, I.-D. *J. Power Sources* **2014**, *248*, 1211−1217.
(21) Wang, H.; Li, H.; Yu, L.; Jiang, Y.; Wang, K. *J. Appl. Polym. Sci.* **2013**, *130*, 2886−2890.
(22) Shin, W.-K.; Lee, Y.-S.; Kim, D.-W. *J. Nanosci. Nanotechnol.* **2013**, *13*, 3705−3710.
(23) Augustin, S.; Hennige, V.; Hörpel, G.; Hying, C. *Desalination* **2002**, *146*, 23−28.
(24) Jia, X.; Li, G.; Yu, Y.; Sui, G.; Liu, H.; Li, Y.; Li, P.; Yang, X. *J. Appl. Polym. Sci.* **2009**, *113*, 283−289.
(25) Mumin, R.; Geng, X.; Liao, Y.; Hu, S.; Li, W. *J. Membr. Sci.* **2012**, *399*, 37−42.
(26) Venugopal, G.; Moore, J.; Howard, J.; Pendalwar, S. *J. Power Sources* **1999**, *77*, 34−41.
(27) Shi, J.-L.; Fang, L.-F.; Li, H.; Zhang, H.; Zhu, B.-K.; Zhu, L.-P. *J. Membr. Sci.* **2013**, *437*, 160−168.

(28) Li, H.; Ma, X.-T.; Shi, J.-L.; Yao, Z.-K.; Zhu, B.-K.; Zhu, L.-P. *Electrochim. Acta* **2011**, *56*, 2641−2647.
(29) Hao, J.; Lei, G.; Li, Z.; Wu, L.; Xiao, Q.; Wang, Li *J. Membr. Sci.* **2013**, *428*, 11−16.
(30) Xiang, H.; Chen, J.; Li, Z.; Wang, H. *J. Power Sources* **2011**, *196*, 8651−8655.
(31) Zhang, M.; Gao, B. *Chem. Eng. J.* **2013**, *226*, 286−292.
(32) Tang, B.; Ge, J.; Zhuo, L.; Wang, G.; Niu, J.; Shi, Z.; Dong, Y. *Eur. J. Inorg. Chem.* **2005**, No. 21, 4366−4369.
(33) Liu, H.; Cao, Q.; Jetal Fu, L.; Li, C.; Wu, Y. P.; Wu, H. Q. *Electrochem. Commun.* **2006**, *8*, 1553−1557.